

Supplementary Materials

of

Drag reduction on micro-trench and micro-post superhydrophobic surfaces underneath a motorboat on the sea

Ning Yu^{1†}, Francisco Jose del Campo Melchor¹, Zhaohui “Ray” Li¹, Jihun Jeon^{1,2}, Jeff D. Eldredge¹, and Chang-Jin “CJ” Kim^{1,3,4}

¹Mechanical and Aerospace Engineering Department, University of California, Los Angeles (UCLA), Los Angeles, California 90095, USA

²Department of Mechanical Engineering, UNIST, Ulsan 44919, Republic of Korea

³Bioengineering Department, University of California, Los Angeles (UCLA), Los Angeles, California 90095, USA

⁴California NanoSystems Institute (CNSI), University of California, Los Angeles (UCLA), Los Angeles, California 90095, USA

† Email address for correspondence: yuning@ucla.edu

S1. Sample Images

In addition to those of sample LT_p100 shown in Figure 6 of the main text, image pairs of samples LT_p75, LT_p50, TT_p100, and AP_p47 taken by a side-view camera and a rear-view camera are shown in Figures S1–S4, respectively.

Similar to LT_p100 in Figure 6, air bubbles at rear end of samples were found on LT_P75 and LT_p50 at low speeds ($U < 4.5$ m/s) and sheared away at high speeds ($U > 4.5$ m/s) in Figures S1 and S2. On all the LT surfaces (i.e., LT_100, LT_p75, and LT_p50), which are the main interest of the paper, the plastron remained pinned (or slightly depinned) to the highest speed of the boat ($U \sim 7.1$ m/s), as shown in Figures 6, S1, and S2.

On TT and AP surfaces, on the other hand, while air bubbles at rear end of samples were also found at low speeds ($U < 4$ m/s) and sheared away at high speeds ($U > 4$ m/s), the plastron started deterioration by depinning-in at slightly higher speeds ($U > 5$ m/s), as shown in Figures S3 and S4. While the plastron on both TT and AP was less stable than on LT as expected, TT fared worse than AP. For example, at the highest speed ($U \sim 7.2$ m/s), the plastron on TT deteriorated over its entire surface (Figure S3) while the plastron on AP deteriorated only on several locations along the sample edges (Figure S4).

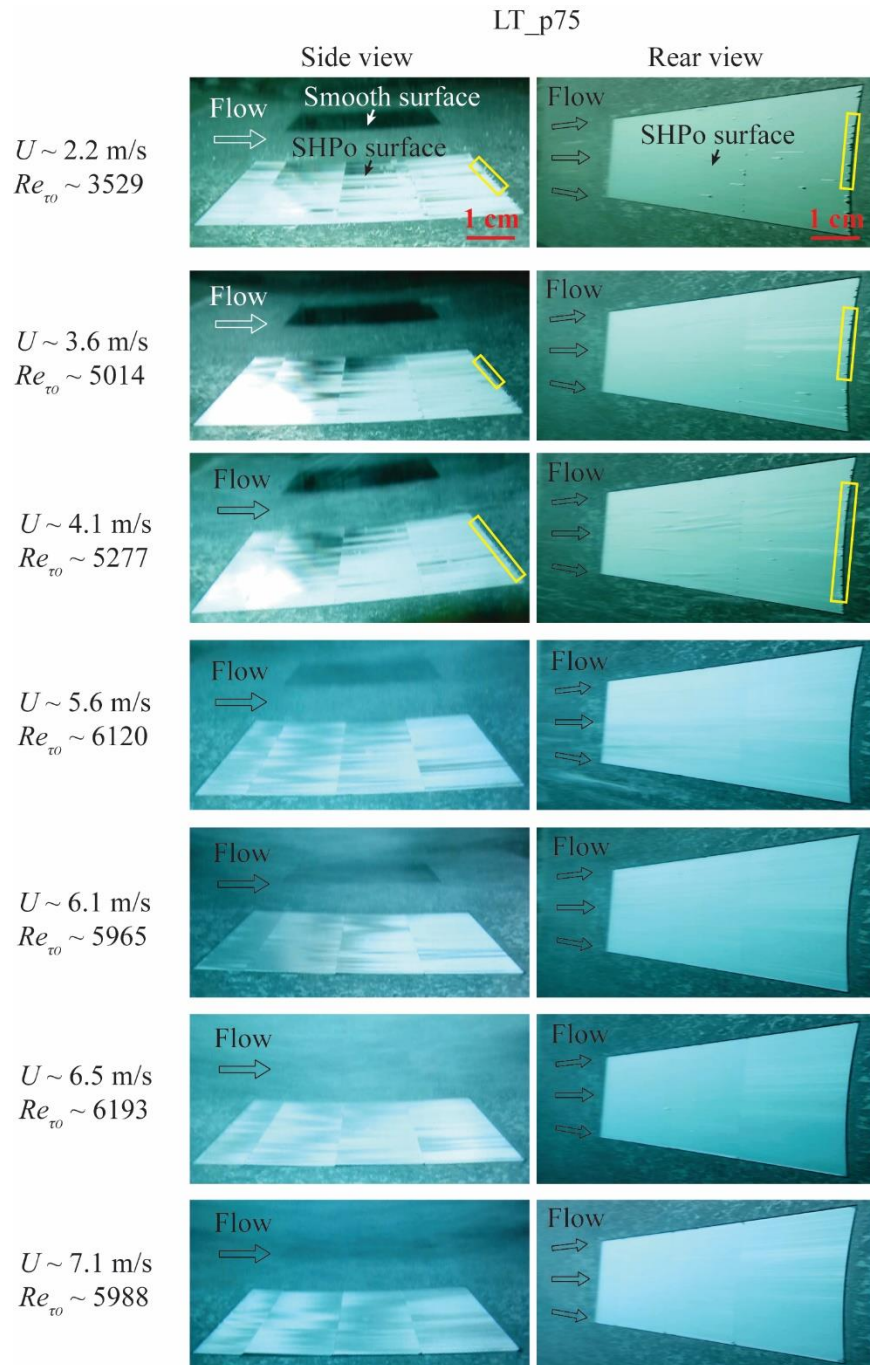


Figure S1. Image pairs of one of the two longitudinal trench samples with the pitch of 75 μm (LT_p75). The images confirm a pinned (including slightly depinned) plastron over the entire trench length up to $U \sim 7.1$ m/s although at low speeds some bubbles were found at the rear end of the sample as identified in the yellow boxes. The dark patches on the surface of the side-view pictures at low speeds are a reflection, not deteriorated plastron, as explained in the main text for Figure 6.

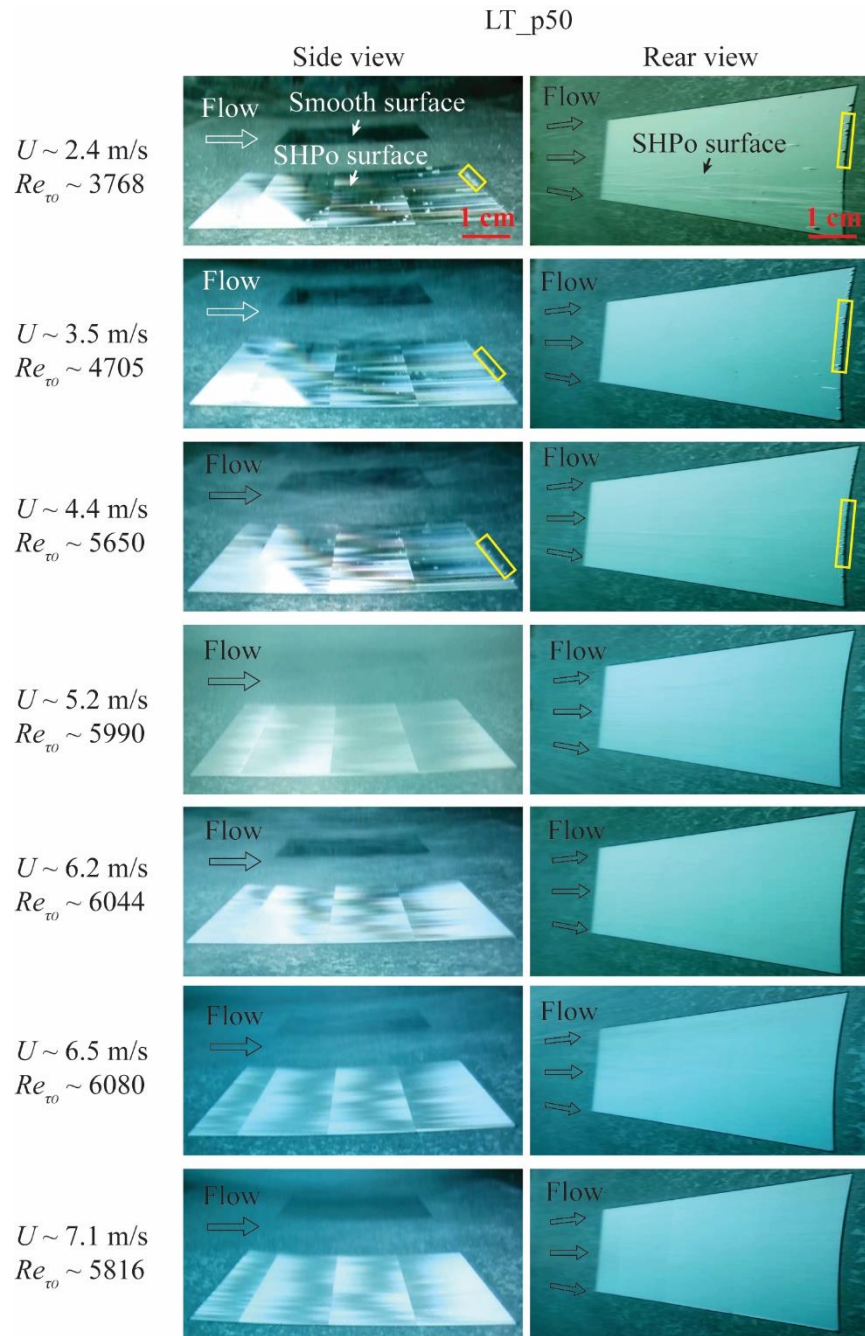


Figure S2. Images pairs of one of the two longitudinal trench samples with the pitch of $50 \mu\text{m}$ (LT_p50). The images confirm a pinned (including slightly depinned) plastron over the entire trench length up to the top speed ($U \sim 7.1$ m/s) although at low speeds some bubbles were found at the rear end of the sample as identified in the yellow boxes. The dark patches on the surface of the side-view pictures at low speeds are a reflection, not deteriorated plastron, as explained in the main text for Figure 6.

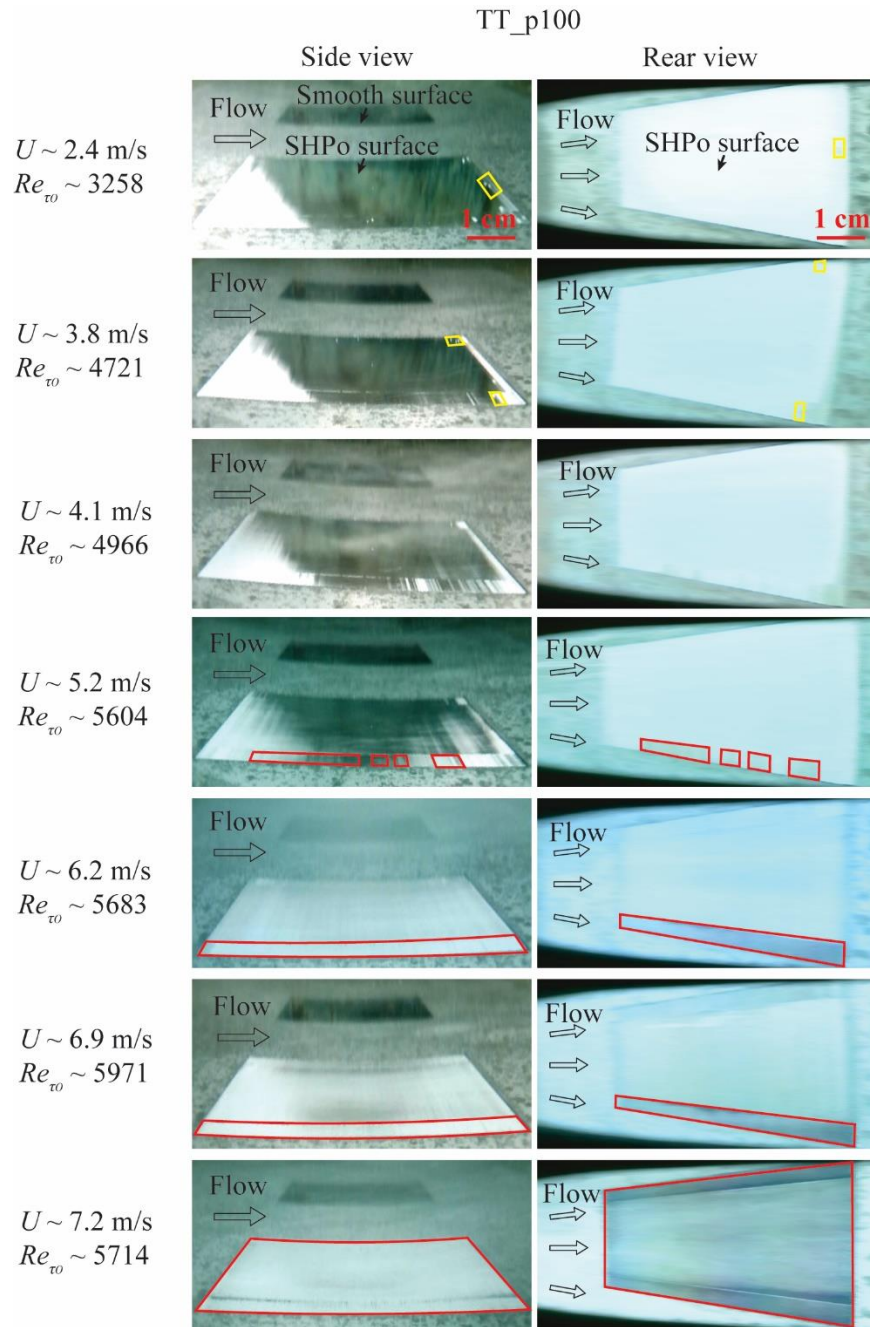


Figure S3. Image pairs of the transverse trench sample with the pitch of $100 \mu\text{m}$ (TT_p100). The images show depinning-in, as outlined by the red boxes, on significant portions of the sample at above $U \sim 6 \text{ m/s}$. At low speeds, some bubbles were found at the rear end of the sample as identified in the yellow boxes. The dark patches on the surface of the side-view pictures at low speeds are a reflection, not deteriorated plastron, as explained in the main text for Figure 6.

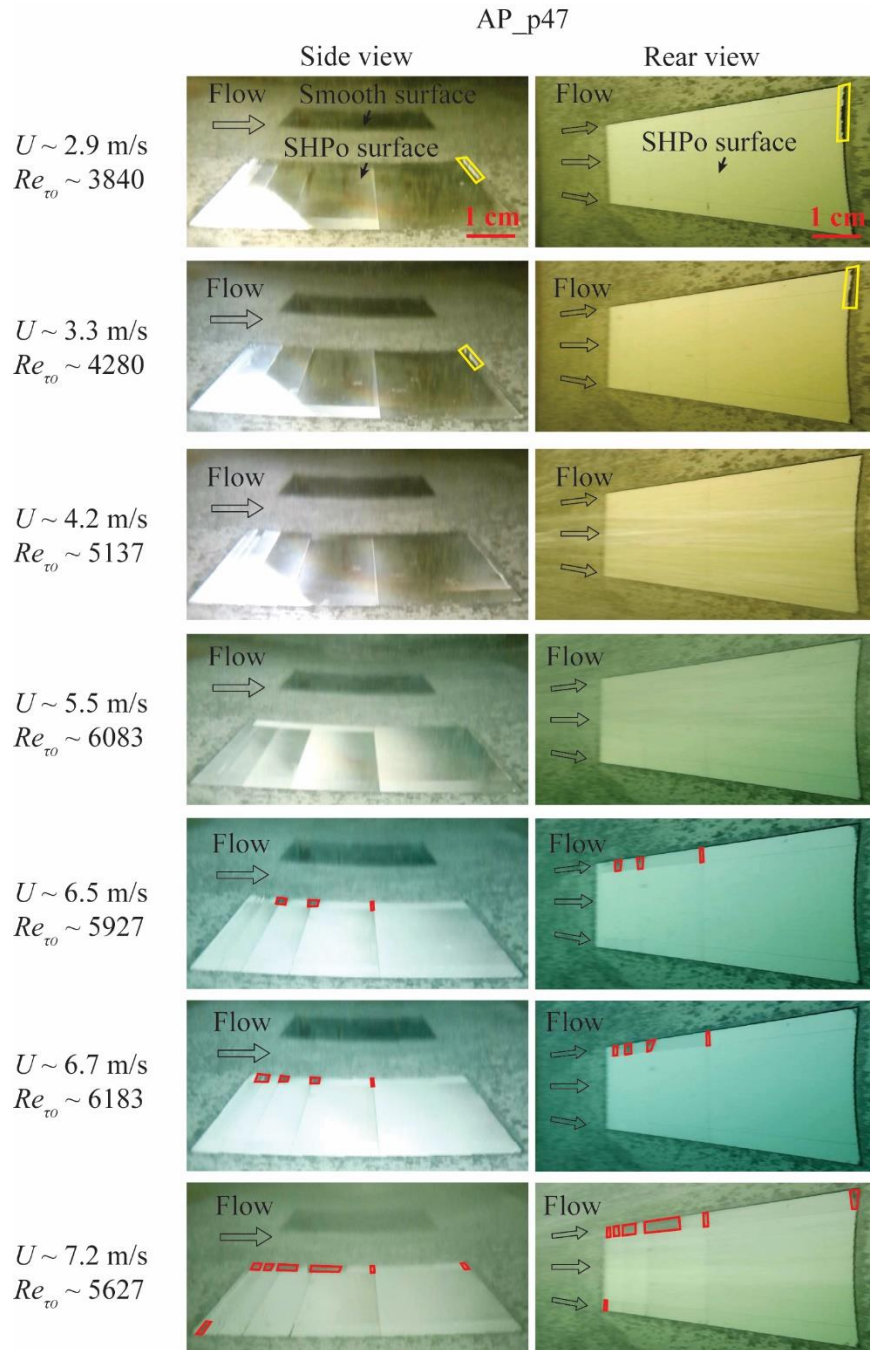


Figure S4. Image pairs of aligned post samples with the pitch of $47 \mu\text{m}$ (AP_p47). The images show depinning-in, as outlined by the red boxes, on several locations of the sample at above $U \sim 6$ m/s. At low speeds, some bubbles were found at the rear end of the sample as identified in the yellow boxes. The dark patches on the surface of the side-view pictures at low speeds are a reflection, not deteriorated plastron, as explained in the main text for Figure 6.

S2. Experimental Data

There were two LT_p100, two LT_P75, two LT_50, one TT_p100, and one AP_p47 samples tested. The entire experimental records are tabulated in Table S1. For each case, the boat speed U , wetting length of the sample x_s , shear stress on the SHPo and smooth surfaces, τ and τ_o , respectively, were measured and averaged for the 40 seconds testing period. The water density and dynamic viscosity at 20 °C, $\rho_{water} = 998 \text{ kg/m}^3$ and $\mu_{water} = 1.0016 \times 10^{-3} \text{ Pa}\cdot\text{s}$ were used to calculate Reynolds numbers. For every case, the plastron status on the sample was monitored with the underwater cameras. Drag measurement data were deemed invalid and discarded if the bubbles are found to cling on the sample or plastron was found deteriorated.

Table S1. Experimental data for each boat test case

Sample	U (m/s)	Re_x	Re_{τ_o}	Re_{τ}	λ^+_o	λ^+	Drag ratio	Valid? (Y/N)
LT_p100	2.9	6.94E+06	4447	4106	6.32	5.83	0.85	N
	3.0	7.22E+06	4479	4064	6.41	5.82	0.82	N
	3.8	9.05E+06	5418	4933	8.11	7.39	0.83	N
	4.1	9.67E+06	5693	5071	8.64	7.70	0.79	N
	4.5	1.04E+07	6111	5246	9.77	8.39	0.74	Y
	5.9	1.11E+07	6095	5101	12.14	10.16	0.70	Y
	4.8	9.98E+06	5730	4932	10.01	8.61	0.74	Y
	5.4	1.10E+07	6136	5193	11.15	9.44	0.72	Y
	6.4	1.11E+07	6118	5025	13.12	10.78	0.67	Y
	6.8	1.13E+07	6206	4909	13.91	11.00	0.63	Y
	6.7	1.11E+07	6195	4970	13.83	11.09	0.64	Y
7.1	1.09E+07	5894	4823	14.21	11.62	0.67	Y	
LT_p100	2.8	6.71E+06	4329	3968	5.95	5.46	0.84	N
	3.3	7.93E+06	4794	4355	6.82	6.19	0.83	N
	4.1	9.75E+06	5572	4885	8.25	7.24	0.77	N
	3.6	8.49E+06	5045	4512	7.43	6.64	0.80	N
	4.0	9.44E+06	5401	4696	8.12	7.06	0.76	N
	4.5	9.40E+06	5465	4671	9.11	7.78	0.73	N
	5.0	9.67E+06	5749	4807	10.37	8.67	0.70	Y
	5.6	1.04E+07	5927	4835	11.37	9.28	0.67	Y
	6.1	1.10E+07	6159	5005	12.42	10.09	0.66	Y
	6.0	1.08E+07	5901	4826	11.86	9.70	0.67	Y
	6.5	1.14E+07	6132	4950	12.86	10.39	0.65	Y
	6.6	1.14E+07	6273	5006	13.17	10.51	0.64	Y
	6.9	1.03E+07	5652	4585	13.50	10.95	0.66	Y
	7.1	1.06E+07	5822	4575	13.97	10.98	0.62	Y
6.9	1.03E+07	5778	4579	13.79	10.93	0.63	Y	

LT_p75	2.2	5.28E+06	3529	3479	3.61	3.56	0.97	N
	2.4	5.71E+06	3775	3697	3.93	3.84	0.96	N
	2.7	6.49E+06	4193	4017	4.48	4.29	0.92	N
	2.9	6.99E+06	4287	4064	4.64	4.40	0.90	N
	3.6	8.49E+06	5014	4766	5.77	5.48	0.90	N
	4.1	9.50E+06	5277	4965	6.21	5.84	0.89	N
	4.4	9.38E+06	5561	5059	7.14	6.49	0.83	N
	4.9	1.05E+07	6075	5365	7.98	7.05	0.78	Y
	4.9	1.05E+07	6117	5463	8.03	7.17	0.80	Y
	5.6	1.07E+07	6120	5434	8.90	7.90	0.79	Y
	6.1	1.08E+07	5965	5201	9.42	8.21	0.76	Y
	5.7	1.08E+07	5972	5272	8.92	7.87	0.78	Y
	6.5	1.09E+07	6193	5370	10.37	8.99	0.75	Y
	6.7	1.03E+07	5715	4990	10.39	9.07	0.76	Y
	7.0	1.07E+07	5835	5019	10.68	9.19	0.74	Y
7.1	1.12E+07	5988	5157	10.72	9.23	0.74	Y	
LT_p75	2.4	5.75E+06	3821	3754	3.61	3.54	0.97	N
	2.7	6.37E+06	4168	4014	4.02	3.87	0.93	N
	3.6	8.52E+06	5128	4971	5.24	5.08	0.94	N
	4.1	9.49E+06	5752	5348	6.13	5.70	0.86	N
	4.7	9.93E+06	5954	5315	7.00	6.25	0.80	Y
	5.3	1.09E+07	6220	5463	7.81	6.86	0.77	Y
	5.5	1.11E+07	6375	5508	8.04	6.95	0.75	Y
	6.4	1.10E+07	6168	5310	9.11	7.84	0.74	Y
	5.2	1.02E+07	5967	5329	7.71	6.88	0.80	Y
	5.7	1.08E+07	6172	5309	8.35	7.19	0.74	Y
	6.5	1.09E+07	6075	5300	9.22	8.04	0.76	Y
	7.2	1.14E+07	6218	5389	10.11	8.77	0.75	Y
	5.6	1.08E+07	6145	5339	8.11	7.05	0.75	Y
6.6	1.11E+07	6286	5501	9.58	8.38	0.77	Y	
6.0	1.07E+07	6059	5275	8.65	7.53	0.76	Y	
LT_p50	3.2	7.57E+06	4734	4683	3.40	3.37	0.98	N
	4.0	9.28E+06	5485	5171	4.20	3.96	0.89	N
	3.8	8.97E+06	5272	5050	4.01	3.84	0.92	N
	3.5	8.23E+06	4705	4597	3.51	3.43	0.95	N
	4.4	9.60E+06	5650	5273	4.61	4.30	0.87	N
	4.3	9.47E+06	5522	5252	4.49	4.27	0.90	N
	5.2	1.08E+07	5990	5589	5.29	4.93	0.87	Y
	5.0	1.03E+07	5883	5454	5.15	4.77	0.86	Y
	6.2	1.15E+07	6044	5576	6.04	5.57	0.85	Y
5.2	1.01E+07	5819	5454	5.38	5.05	0.88	Y	

	6.4	1.11E+07	6153	5609	6.56	5.98	0.83	Y
	7.0	1.17E+07	6127	5485	6.88	6.16	0.80	Y
	6.5	1.08E+07	6080	5445	6.72	6.02	0.80	Y
	7.0	1.07E+07	5697	5188	6.81	6.20	0.83	Y
	7.1	1.09E+07	5816	5254	6.99	6.31	0.82	Y
LT_p50	2.1	5.07E+06	3403	3380	2.12	2.11	0.99	N
	2.6	6.10E+06	3937	3870	2.55	2.51	0.97	N
	3.1	7.33E+06	4508	4371	3.03	2.94	0.94	N
	3.9	9.11E+06	5307	5107	3.80	3.66	0.93	N
	4.1	9.59E+06	5544	5352	4.01	3.88	0.93	N
	4.9	1.05E+07	5941	5650	4.79	4.56	0.90	Y
	4.6	9.88E+06	5729	5293	4.56	4.22	0.85	Y
	5.2	1.11E+07	6085	5677	4.96	4.63	0.87	Y
	6.8	1.04E+07	5673	5135	6.35	5.75	0.82	Y
	6.9	1.05E+07	5754	5229	6.45	5.86	0.83	Y
	7.2	1.07E+07	5692	5135	6.57	5.93	0.81	Y
	5.8	1.10E+07	6063	5602	5.58	5.16	0.85	Y
	7.4	1.08E+07	5703	5118	6.73	6.04	0.81	Y
	6.5	1.08E+07	5934	5362	6.17	5.57	0.82	Y
TT_p100	3.4	8.15E+06	5017	5180	3.78	3.90	1.07	N
	3.2	7.61E+06	4634	4834	3.44	3.59	1.09	N
	3.2	7.62E+06	4820	4946	3.58	3.67	1.05	N
	3.7	8.17E+06	5098	5138	4.10	4.13	1.02	Y
	4.0	8.90E+06	5446	5519	4.45	4.51	1.03	Y
	4.3	9.47E+06	6021	5940	5.10	5.03	0.97	Y
	5.3	1.10E+07	6253	6234	5.72	5.70	0.99	Y
	5.5	1.04E+07	5861	5988	5.86	5.99	1.04	Y
	6.0	1.07E+07	6096	6210	6.48	6.60	1.04	Y
	6.3	1.15E+07	6260	6894	6.56	7.22	1.21	N
6.0	1.08E+07	6093	6384	6.48	6.79	1.10	N	
AP_p47	2.2	5.22E+06	3267	3422	2.28	2.39	1.10	N
	2.2	5.30E+06	3555	3549	2.49	2.49	1.00	N
	3.3	7.93E+06	4839	4584	3.68	3.48	0.90	N
	2.9	6.96E+06	4473	4257	3.31	3.15	0.91	N
	3.0	7.05E+06	4426	4193	3.29	3.11	0.90	N
	3.7	8.25E+06	4885	4703	3.99	3.84	0.93	Y
	4.2	9.19E+06	5532	5256	4.73	4.49	0.90	Y
	4.4	9.41E+06	5627	5369	4.94	4.72	0.91	Y
	4.8	9.99E+06	6004	5703	5.47	5.19	0.90	Y
	4.6	9.55E+06	5579	5325	5.03	4.80	0.91	Y
5.5	1.03E+07	6185	5835	6.26	5.91	0.89	Y	

5.7	1.07E+07	6015	5794	6.14	5.91	0.93	N
5.7	1.05E+07	5879	5575	6.14	5.83	0.90	N
6.2	1.11E+07	6145	6001	6.67	6.51	0.95	N
6.4	1.14E+07	6410	6390	7.00	6.98	0.99	N
6.0	1.10E+07	6188	5877	6.52	6.19	0.90	N
6.5	1.16E+07	6173	6049	6.76	6.62	0.96	N
6.5	1.16E+07	6215	6136	6.80	6.71	0.97	N